Dispersion Polymerization of Vinylidene Fluoride in Supercritical Carbon Dioxide

Philipp A. Mueller,† Giuseppe Storti, and Massimo Morbidelli*

Swiss Federal Institute of Technology Zurich, ETHZ Institut für Chemie- und Bioingenieurwissenschaften, ETH−Hönggerberg/HCI, CH-8093 Zurich, Switzerland

Ivano Costa, Alessandro Galia, Onofrio Scialdone, and Giuseppe Filardo

University of Palermo, Dipartimento Ingegneria Chimica Processi e Materiali, Viale delle Scienze, I-90128 Palermo, Italy

Received May 2, 2006; Revised Manuscript Received July 12, 2006

ABSTRACT: The dispersion polymerization of vinylidene fluoride in supercritical carbon dioxide is investigated using two ammonium carboxylate perfluoropolyether stabilizers of different molecular weights. Under suitable operating conditions a polymer made of well-dispersed spherical particles has been obtained up to relatively high conversion. The experimental data of polymerization rate and molecular weight distribution are in good agreement with the predictions of a model previously developed. Such an agreement supports the conclusion that the polymerization kinetics is dominated by the interphase transport of the active radicals between the continuous phase and the polymer particles.

1. Introduction

Increasing concern for the negative environmental impact of volatile organic compounds and organic-containing aqueous wastes produced by conventional polymerization of unsaturated monomers has induced a search for alternative polymerization media. The use of supercritical carbon dioxide ($scCO_2$) represents probably the most attractive one. Many research groups reported in fact the successful polymerization of a number of vinyl monomers in $scCO_2$ during the past decade,[1−3] and DuPont recently introduced the first commercial fluoropolymers manufactured in $scCO_2$.[4]

Vinylidene fluoride (VDF) has been successfully polymerized in $scCO_2$ in the absence of stabilizers (i.e., by precipitation polymerization) both in continuous[5−8] as well as in batch reactors.[9,10] In these experiments, the polymer has been obtained in the form of a white powder made of irregular, unshaped particles with broad size distribution. The microstructure of the PVDF produced in $scCO_2$ has been reported to exhibit anomalous characteristics. In particular, bimodal molecular weight distributions (MWDs) have been observed under certain reaction conditions. These findings, not fully consistent with previous models of heterogeneous polymerization in $scCO_2$,[11] have been recently explained in terms of interphase transport of active polymer chains.[10]

The use of efficient surface-active agents improves significantly the quality of the final polymer by preventing particle coagulation and leading to the formation of a dispersed system with a large interface surface and particles with regular morphology. Under these conditions, several advantages are obtained such as faster polymerization rate, less reactor fouling (which is particularly important in the case of continuous processes), and narrower MWD.

Tai et al.[12] polymerized VDF in $scCO_2$ using poly(dimethylsiloxane) macromonomer (PDMS-mMA) as stabilizer. The scanning electron microscopy (SEM) pictures of the PVDF produced in these experiments indicate that this stabilizer is not particularly effective for this specific polymerization system. Only a limited improvement of the polymer particle morphology is in fact observed with respect to the case of precipitation polymerization. The same group investigated also the performance of a fluorinated graft maleic anhydride copolymer stabilizer.[13] Although a polymer with better morphology was obtained, the particles appeared to be strongly attached to each other and even partly interfused. Moreover, this stabilizer seems to be effective only at low monomer conversion (<15%).

Recently, it has been shown that effective stabilization at high monomer conversions can be obtained using ammonium carboxylate perfluoropolyether stabilizers.[14] Using these compounds and suitable experimental conditions, PVDF was obtained at high rates with yields higher than 60% in the form of microspheres.

Besides its obvious interest due to the efficiency of the reaction and the characteristics of the final product, this process provides new insights into the kinetics of heterogeneous supercritical polymerization due to the particularly large interphase surface areas achieved. Mueller et al.[10] identified in fact the interphase transport of radical chains to be the key process responsible for the occurrence of bimodal MWDs in PVDF produced by precipitation polymerization in $scCO_2$. According to the mechanism proposed in that work, a significant increase of the interphase surface area (which is definitely the case when moving from precipitation polymerization to a stable dispersion polymerization with well-defined micron-sized particles) would affect the shape of the MWD of the produced polymer, possibly suppressing its peculiar bimodality. Thus, in addition to developing an efficient stabilization system for VDF polymerized in $scCO_2$, the aim of this work is to combine experimental data and model simulations for two specific stabilizers so as to check the reliability of the proposed reaction mechanism together with the possibility of controlling the presence of a bimodality in the MWD.

* To whom correspondence should be addressed. E-mail: massimo.morbidelli@chem.ethz.ch. Telephone +41-1-6323034. Fax: +41-1-6321082.

† Actual address: DuPont Engineering Research and Technology (DuET) Experimental Station, P.O. Box 80249, Wilmington, DE 19880-0249.

10.1021/ma060981l CCC: $33.50
Published on Web 08/19/2006

Table 1. Ammonium Carboxylate Perfluoropolyether Stabilizers Used in This Work

stabilizer[a]	code	M_w [g mol^{-1}]	n range
$Cl-(CF_2CF(CF_3)O)_nCF_2COO^- NH_4^+$	FLK 7850A	500	2−4
	FLK 7004A	1000	2−6

2. Experimental Section

2.1. Materials. Vinylidene fluoride monomer was kindly donated by Solvay Solexis (Bollate, Italy), CO_2 was from Air Liquide, 99.998% pure. Both chemicals were used without further purification. The DEPDC initiator was synthesized according to a procedure described in the literature[15] by using water as the solvent and extracting the peroxydicarbonate into Freon 113 (HPLC grade). The concentration of active peroxide in the solution was determined by iodine titration technique, ASTM method E 298−91. All manipulations of the initiator solution were performed at 0 °C, and the final product was stored under dark at −22 °C. Two perfluoropolyether salts, with different molecular weights, have been tested as stabilizers and supplied by Solvay Solexis. Their structures are reported in Table 1, where the correspondence with their conventional code is also given. All of them have a water content ranging between 1 and 2% w/w. Prior to utilization, the stabilizers were dried under vacuum for one night at 50 °C to decrease the water content. All other chemicals were obtained from Aldrich and used as received.

2.2. Apparatus. Polymerization experiments were carried out in an AISI 316 fixed-volume (ca. 26 cm^3) batch reactor, equipped with pressure transducer and Pt 100 temperature sensor. The reaction mixture was stirred by a magnetic bar, and the reactor was logged to the automated temperature control system described elsewhere.[16]

2.3. Polymerization Procedure. The dried surfactant and the initiator, the latter in the form of a liquid solution in Freon 113, were first charged in the reactor. The vessel was then purged by a controlled flow rate of CO_2 maintained for at least 20 min to remove oxygen and volatile Freon. After sealing the reactor, liquid VDF and CO_2 were added at room temperature by using two different ISCO syringe pumps. The total amounts of solvent and monomer introduced were measured by weighing the vessel using an electronic balance (Sartorius, max 8 kg, precision 0.01 g). When the desired value of nominal density of the polymerization mixture was reached (estimated as the ratio of the total mass of CO_2 and VDF to the reactor volume), the vessel was inserted in the control system and heated to the reaction temperature (50 °C), while the acquisition of temperature, T_r and pressure, p of the polymerization mixture, along with the temperature of the heating water bath, T_w, was started. The time needed to reach the desired temperature value was always less than 20 min. Such a short thermal transient, together with the long half-life time of the selected initiator in these conditions, result in negligible consumption of initiator before the final operating temperature is achieved.

At the end of the polymerization, the reactor was rapidly cooled by immersion in an ice and water bath and slowly depressurized by bubbling the outlet gas in tetrahydrofurane in order to trap solid polymer possibly entrained by the fluid stream. Part of the collected polymer was extracted soon after the polymerization experiment with supercritical carbon dioxide at 40 °C and 200 bar for 4 h in order to remove the stabilizer before any further characterization. The reliability of this procedure has been discussed by Scialdone et al.[17]

2.4. Analytical Techniques. To investigate the time evolution of the reaction, experiments with the same recipe and under identical conditions have been carried out and stopped at different reaction times. The amount of polymer produced was estimated by gravimetry, and the complete MWD was measured by gel permeation chromatography (GPC). These measurements were performed using solutions of PVDF at about 3 g L^{-1} in *N*,*N*-dimethylacetamide (DMA, HPLC quality grade), modified with 0.1 mol L^{-1} LiBr under heating (60 °C), and stirred for 30 min. A Hewlett-Packard 1100 series separation module equipped with refractive index as well as UV detectors was used at 45 °C, flow rate of 0.7 mL min^{-1}, and injected sample volume of 75 μL. The bench of columns was made of two Hewlett-Packard 5μ-PLgel mixed-c type columns and one Polymer Laboratories OligoPore column. The molecular weight analysis was based on the universal calibration procedure, using polystyrene (PS) narrow standards (Polymer Laboratories) and the following values of the Mark−Houwink constants: $K = 1.3 \times 10^{-4}$ dL g^{-1}, $a = 0.69$ for PS;[18] $K = 4.5 \times 10^{-4}$ dL g^{-1}, $a = 0.70$ for PVDF.[19]

Particle morphologies were analyzed with a Philips scanning electron microscope (SEM). Samples were sputter-coated with gold to a thickness of 200 Å. The particle size distributions (PSDs) were evaluated by measuring the diameters, D_i of at least 100 individual particles through a software for image analysis of micrographs, then number-average particle size, D_n and polydispersity, D_w/D_n were determined as detailed elsewhere.[16]

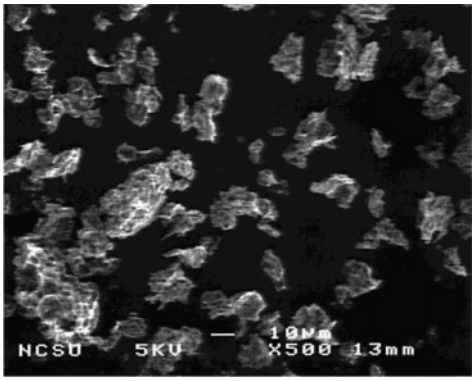

Figure 1. SEM picture of PVDF powders produced by precipitation polymerization in scCO$_2$.[8]

3. Results and Discussion

The precipitation polymerization of VDF in scCO$_2$ produces a polymer in the form of a white powder. Its morphology is characterized by irregular particles of different shapes and sizes. Figure 1 shows a typical SEM picture of such a powder.[8] It is seen that particle diameters much larger than 10 μm are obtained. Better-defined particles have been achieved when polymerizing VDF in the presence of PDMS-mMA or a fluorinated graft stabilizer (cf. SEM pictures in refs 12, 13). Although some submicron-sized particles can be identified in this case, most of them appear partly interfused and not well dispersed.

A significant improvement in the particle morphology was achieved when ammonium carboxylate perfluoropolyether salts were used as stabilizers.[14] The produced polymer particles are shown in Figure 2, at different magnifications, for the two stabilizers considered and different conversion values. This is the first dispersion of well-defined spherical particles obtained by polymerizing VDF in scCO$_2$. The final average particle diameter is about 2 μm, a value similar to the one obtained through dispersion polymerization of amorphous polymers such as poly(methyl methacrylate)[20,21] or poly(styrene).[22] It is worth noting that the SEM pictures shown in Figure 2 were taken at relatively large monomer conversions, i.e., from 41 to 61%, thus indicating the effectiveness of the stabilizer during the entire reaction. Moreover, the solid content of the polymerization medium was about 200 g L^{-1}, which is significantly larger than that used to test the performance of the fluorinated graft maleic anhydride copolymer stabilizer discussed above.

According to the mechanism proposed by Mueller et al.,[10] the interphase surface area is a key quantity in heterogeneous polymerization in scCO$_2$. To estimate the degree of segregation

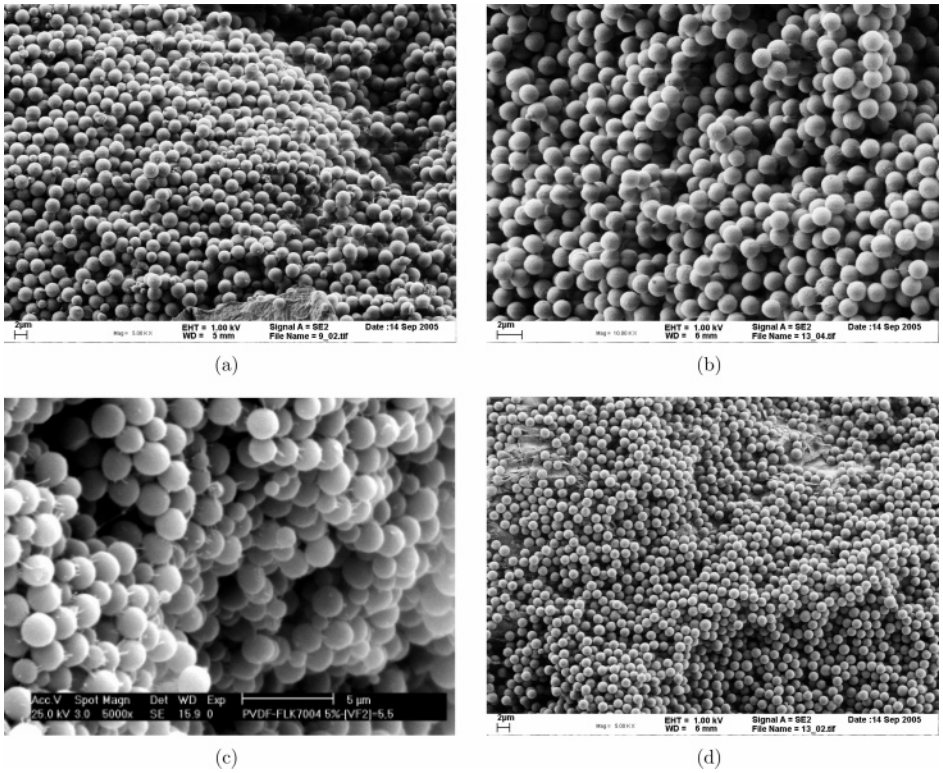

Figure 2. SEM picture of PVDF powders produced by dispersion polymerization in $scCO_2$ under the conditions reported in Table 2 and different stabilizer (FLK 7850A and FLK 7004A, see Table 1) and conversion value: (a) FLK 7850A, $X = 45\%$; (b) FLK 7850A, $X = 61\%$; (c) FLK 7004A, $X = 41\%$; (d) FLK 7004A, $X = 50\%$.

in a two-phase polymerization system, the so-called Ω parameter has been introduced.[10,23,24] This quantity is defined as the ratio between the characteristic times of termination within a specific phase and interphase mass transport outside the phase, respectively:

$$\Omega_{x,j} = \frac{K_{x,j} A_p}{k_{t,j}[R_j] V_j} \tag{1}$$

$K_{x,j}$ being the overall mass-transfer coefficient of a chain of length x referred to phase j according to the two-film theory, A_p the total particle surface area, $k_{t,j}$ the termination rate constant in phase j, $[R_j]$ the total radical concentration in phase j, and V_j the volume of phase j. Accordingly, Ω values much smaller than one indicate radical segregation within the phase, that is, the radical terminates inside the phase before being able to diffuse to the other phase, whereas in the opposite case, the active chains will diffuse to the other phase.

For the polymerization of most vinyl monomers in $scCO_2$, the value of the Ω parameter in the polymer phase, Ω_{pol} is always well below one and approaches zero quite fast at increasing chain lengths.[23] Thus, to analyze the extent of segregation of such polymerization systems, it is enough to consider the Ω values in the continuous phase, Ω_{sc}. For chains containing more than a few tens of monomer units (i.e., most of the polymer chains), the effect of the chain length on the involved parameters becomes negligible and eq 1 reduces to the following simplified expression:[23,24]

$$\Omega_{sc} \approx \frac{\bar{D}_{sc} A_p}{\delta_{sc} k_{t,sc}[R_{sc}] V_{sc}} \tag{2}$$

where $\bar{D}_{sc}$ denotes the diffusion coefficient of chains of length equal to the average value characteristic of the continuous phase and δ_{sc} is the characteristic length of interphase diffusion. The average degree of polymerization of chains in the continuous phase was roughly estimated from the position of the low-molecular-weight mode in experimentally measured MWDs for the same system (cf. Figure 4 in ref 10) and set equal to 700. The film thickness, δ_{sc}, in a dispersion of small particles under gentle stirring, can be approximated to the particle radius. Thus, using typical parameter values (cf. Table 3), an Ω_{sc} value slightly larger than 400 is obtained for VDF dispersion polymerization under the conditions reported in Table 2. Note that the value of the total radical concentration, $[R_{sc}]$, reported in Table 3, has been estimated from the following balance assuming pseudo steady state:

$$\frac{d[R_{sc}]}{dt} = 2 f_{sc} k_{d,sc}[I_{sc}] - k_{t,sc}[R_{sc}]^2 - \frac{\bar{D}_{sc}}{r_p}\frac{A_p}{V_{sc}}[R_{sc}] \approx 0 \tag{3}$$

Table 2. Polymerization Recipe and Operating Conditions

T, °C	50
p_0, bar	380
stirring, rpm	300
$[M]_0$, mol cm^{-3}	5.4×10^{-3}
$[I]_0$, mol cm^{-3}	5.5×10^{-6}
m^0_{FLK}, g (5% w/w)	0.45

Table 3. Typical Values of the Parameters in Eq 2 for the VDF Polymerization in $ScCO_2$ under the Conditions Reported in Table 2

parameter	value
V_{sc}, cm^3	26
A_p, cm^2	9.2×10^4
δ_{sc}, cm	1.0×10^{-4}
$k_{t,sc}$, $cm^3\ mol^{-1}\ s^{-1}$	8.0×10^{12}
$\bar{D}_{sc}$, $cm^2\ s^{-1}$	2.3×10^{-5}
$[R_{sc}]$, mol cm^{-3}	2.4×10^{-13}

the first term on the right-hand side being the radical production term by initiator decomposition and the other two the loss terms due to bimolecular termination and interphase transport, respectively.

The value of Ω_{sc} estimated above is well above unity, which means that, most probably, the radical chains initiated in the continuous phase diffuse into the particles where they terminate (because $\Omega_{pol} < 1$). Thus, having $\Omega_{sc} \gg 1$ and $\Omega_{pol} \ll 1$ indicates that polymerization occurs mainly in the polymer phase, i.e., we have a single polymerization locus. The same situation has been observed in the case of methyl methacrylate (MMA) dispersion polymerization in $scCO_2$.[23,24] In this case, a typical monomodal MWD, characterized by high molecular weights, is obtained.

The model used for the quantitative comparison with the experimental data discussed in the following has originally been developed by Mueller et al.[10,24] This is a comprehensive, generalized kinetic model of heterogeneous polymerization in $scCO_2$, whose main characteristics are as follows: (1) Two reaction loci are considered: the polymer-rich dispersed phase and the CO_2-rich continuous phase. (2) Low-molecular-weight species (solvent, initiator, and monomer) undergo very fast transport between the phases and are therefore assumed to be at equilibrium conditions at all times. For larger-molecular-weight species, the interphase mass transport is described. (3) A chain-length-dependent partition coefficient for polymer chains between continuous and dispersed phase is considered. (4) The process of particle formation or nucleation is not simulated, and a constant number of spherical particles is assumed throughout the entire process. This is because the nucleation period where the particle number changes significantly is expected to be very short in these systems.[25,26] (5) The crystalline part of the polymer is assumed to be impermeable to all species and therefore neglected when evaluating interphase partitioning of the various species. The interphase equilibrium partitioning of monomer and CO_2 was described by the Sanchez−Lacombe equation of state, whereas a constant partition coefficient has been used for the initiator. Population balance equations have been derived for the radical and terminated chains in both phases and numerically solved using the method proposed by Kumar and Ramkrishna.[27−29] More details about the derivation of the equations and the numerical solution can be found elsewhere.[10,23,24]

Before comparing the experimental results with the model predictions, it is worth discussing the model parameter evaluation. The same parameter values as in ref 10 have been used, with the exception of the termination rate constant in the polymer phase, $k_{t,pol}$, which has been slightly adjusted. In particular, the reaction radius, r_{xy} (i.e., the separation distance at which the termination between two radical chains of length x and y is instantaneous) has been calculated as the geometric average of the two limiting values given by the Lennard-Jones diameter of the monomer and the distance of the chain end from the closest node of entanglement, respectively (cf. eqs 55−57 in ref 23). In the previous paper,[10] the arithmetic average had been used. However, because the particle surface area A_p was considered there as an adjustable parameter, and the two parameters appear in the model only through their product ($r_{xy}A_p$), the estimation of r_{xy} was actually not relevant. On the other hand, in this work, the value of A_p is measured experimentally. Because in fact a stable dispersion of spherical particles with narrow size distribution has been obtained, it is possible to estimate the final particle radius, r_p^f from the pictures in Figure 2 and the corresponding value of the particle

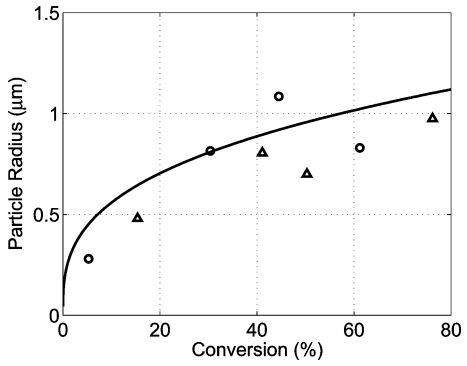

Figure 3. Particle radius as a function of conversion for the operating conditions reported in Table 2. Experimental data: FLK 7850A (○) and FLK 7004A (△). Model: solid line.

number (which is an input quantity for the model) from the following equation:

$$N_p = \frac{3X^f m^0_{VDF}}{4\pi\rho_{PVDF} r_p^{f3}} \tag{4}$$

where X^f denotes the conversion at which r_p^f has been evaluated, m^0_{VDF} is the initial monomer mass, and ρ_{PVDF} is the density of the polymer. Finally, assuming a constant particle number, the total particle surface area, A_p, is evaluated as a function of conversion as follows:

$$A_p = 4\pi\left(\frac{3V_{pol}}{4\pi N_p}\right)^{2/3} N_p \tag{5}$$

The volume of the polymer phase, V_{pol}, is, of course, a function of conversion and is estimated accounting for the actual phase composition as predicted by the Sanchez−Lacombe equation of state.

It is worth noting that the direct experimental evaluation of the particle surface through eqs 4 and 5 is a major difference with respect to the previous work.[10] This increases significantly the predictive level of the simulations reported below, where no parameter is in fact adjusted to fit the experimental data.

Figure 3 shows a comparison between calculated and experimentally observed particle radius as a function of conversion for the two considered stabilizers. Note that the values at high conversion are well reproduced because, as discussed above, the particle number given as input to the model has been estimated so as to fit such data. On the other hand, the good description of the evolution of the particle size over the entire conversion range is a clear confirmation of the assumption of constant particle number all along the reaction. This indicates that the particle nucleation interval is indeed very short and limited to the very beginning of the reaction. This finding is in agreement with the results by Fehrenbacher et al.[25,26] for the system MMA-PDMSmMA, where nucleation was estimated to be over by less than 0.1% conversion. In addition, the data in Figure 3 indicate that the performance of the two stabilizers is comparable, the time evolution of the average particle size in both cases being almost identical. Because this is the only quantity that is affected by the type of surfactant in this model, it follows that we cannot distinguish between the two stabilizers in the model simulations. Accordingly, the experiments conducted with different stabilizer but otherwise identical conditions are compared with the same model predictions in the following.

The pressure values as a function of conversion are shown in Figure 4. The reasonable agreement between predictions and

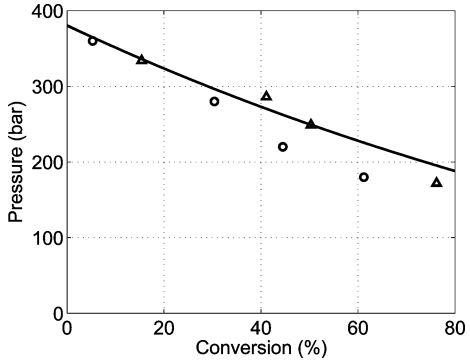

Figure 4. Pressure as a function of conversion for the operating conditions reported in Table 2. Experimental data: FLK 7850A (○) and FLK 7004A (△). Model: solid line.

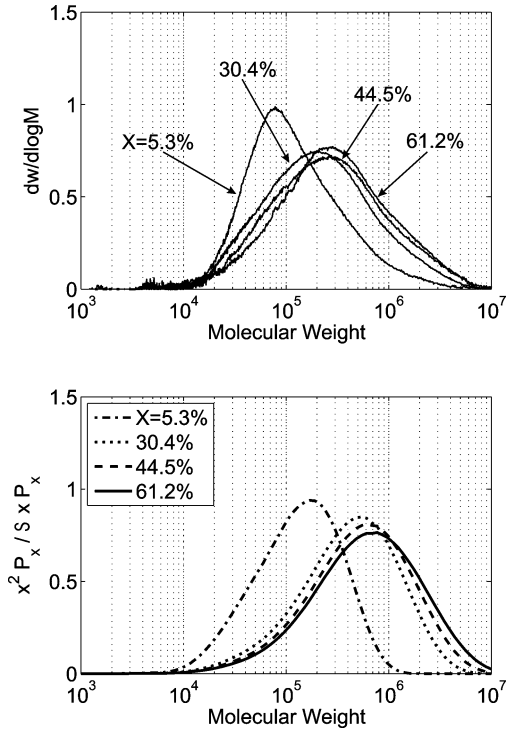

Figure 5. Experimental (a) and predicted (b) molecular weight distributions at various conversions for the operating conditions reported in Table 2.

measurements shows the reliability of the selected equation of state. At first sight, the decrease of pressure during reaction is not surprising because of the larger molar volume of VDF with respect to that of the corresponding polymer. However, an increase of pressure has also been observed for different polymerization systems depending on the initial pressure value.[20] Lepilleur and Beckman[30] explained this behavior with the nonideality of the monomer/CO_2 mixture. Positive pressure changes were observed only at very low initial pressure values because the nonideal contributions become less important at higher initial values due to the liquidlike behavior of CO_2. This behavior is exhibited also by the system considered.

Following the preliminary Ω analysis reported above, it is now interesting to compare experimental findings and model results in terms of MWD and polymerization rate. The former is shown in Figure 5 as a function of conversion. Some deviations between predicted and measured distributions are present, in particular at the lowest conversion value, where the amount of polymer at high molecular weight is underestimated. This discrepancy reflects some limited difference in terms of

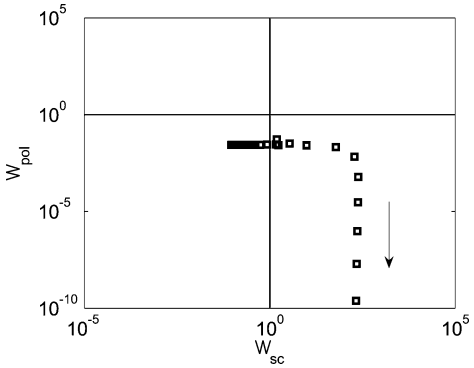

Figure 6. Ω trace calculated at the operating conditions reported in Table 2; the arrow indicates the direction of increasing chain length.

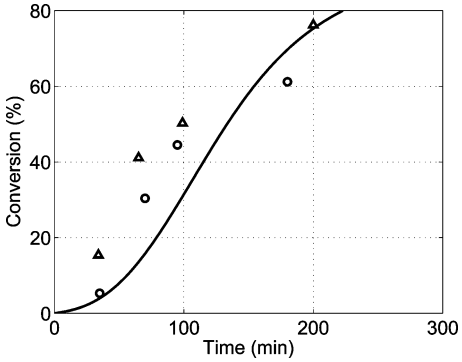

Figure 7. Conversion as a function of time at the operating conditions reported in Table 2. Experimental data: FLK 7850A (○) and FLK 7004A (△). Model: solid line.

time of shift from one dominant reaction locus (the continuous phase) to the other one (the polymer particles). However, the general agreement is quite nice and convincing. In the first place, the predicted monomodal MWD is also found experimentally, which strongly confirms the mechanism of heterogeneous polymerization in $scCO_2$ previously proposed.[10] The detailed Ω trace computed by the complete model (i.e., the Ω values at increasing chain length, following the arrow) is shown in Figure 6 and provides the ultimate explanation of the experimental observations. As expected from the preliminary analysis reported above, the Ω values are clearly larger than one for most of the active chains in the continuous phase, similar to other systems considered in previous studies.[23,24] This means that radicals initiated in the supercritical phase will diffuse into the particles rather than terminate in the former. Because the Ω values in the polymer phase are (as usual) well below one, the entering active chains will most probably further propagate and finally terminate within the particles. This situation leads to the formation of one single population of polymer chains characterized by the conditions prevailing within the polymer phase, as confirmed by the monomodal MWD.

In Figure 7, the predicted conversion values are compared with those measured experimentally as a function of time. Once more, a reasonable agreement is found, even though the reaction rate is significantly larger than the one observed previously in the case of precipitation polymerization,[10] under which conditions the model parameter values have been estimated. This acceleration is expected because, in the experiments carried out in the frame of this work, the main portion of the polymer was produced in the particles where, due to the high viscosity, termination is significantly suppressed, leading to increased radical concentration.

4. Conclusions

VDF has been successfully polymerized in $scCO_2$ via dispersion polymerization. The selected stabilizers (FLK 7850A and FLK 7004A), previously proved to give well-defined micron-sized spherical particles of PVDF in $scCO_2$,[14] were shown to be effective up to large conversion values. The obtained experimental results are in good agreement with model predictions, thus providing a confirmation of the mechanistic picture of heterogeneous polymerization in $scCO_2$ proposed previously.[10] This confirmation is even stronger when considering that all model parameters have been estimated from independent experimental information or sources, without any fitting to the conversion and MWD values measured in this work.

Acknowledgment. The financial support of BBW (Swiss Federal Office for Education and Science, contract no. 02-0131) and EU (growth program ECOPOL project contract no. G1RD-CT-2002-00676) is gratefully acknowledged. P.M., G.S., and M.M. also acknowledge ETH (ETHZ internal research project "Dispersion Polymerization in Supercritical Carbon Dioxide").

Notation

a = Mark−Houwink constant
A_p = total particle surface area, cm^2
D_i = particle diameter, cm
D_n = number-average particle diameter, cm
D_w = weight-average particle diameter, cm
$\bar{D}_{sc}$ = diffusion coefficient of chains of average length in continuous phase, $cm^2\ s^{-1}$
f_j = initiator efficiency in phase j
$[I]_0$ = overall initial initiator concentration, mol cm^{-3}
$[I_j]$ = initiator concentration in phase j, mol cm^{-3}
$k_{d,j}$ = initiator decomposition rate constant in phase j, s^{-1}
$k_{t,j}$ = termination rate constant in phase j, $cm^3\ mol^{-1}\ s^{-1}$
K = Mark−Houwink constant, dL g^{-1}
$K_{x,j}$ = overall mass-transfer coefficient of a chain of length x referred to phase j, cm s^{-1}
m_i^0 = initial mass of component, i, g
$[M]_0$ = overall initial monomer concentration, mol cm^{-3}
N_p = particle number
p = pressure, bar
r_p = particle radius, cm
r_p^f = particle radius measured at conversion X^f, cm
r_{xy} = separation at which termination between chains of length x and y is instantaneous, cm
$[R_j]$ = total concentration of radical chains in phase j, mol cm^{-3}
t = time, s
T = temperature, °C
T_r = reactor temperature, °C
T_w = water bath temperature, °C
V_j = volume of phase j, cm^3
x, y = degree of polymerization
X = monomer conversion
X^f = monomer conversion at which r_p^f has been taken

Greek Letters

δ_j = film thickness in phase j, cm
ρ_i = density of component, i, g cm^{-3}
$\Omega_{x,j}$ = ratio between characteristic times of termination and interphase mass transport of a chain of length x in phase, j, cf. eq 1

References and Notes

(1) Canelas, D. A.; DeSimone, J. M. Polymerizations in Liquid and Supercritical Carbon Dioxide. In *Metal Complex Catalysts Supercritical Fluid Polymerization Supramolecular Architecture*; Springer-Verlag: New York, 1997; Vol. 133.
(2) Ajzenber, N.; Trabelsi, F.; Recasens, F. *Chem. Eng. Technol.* **2000**, *23*, 829−839.
(3) Cooper, A. I. *J. Mater. Chem.* **2000**, *10*, 207−234.
(4) McCoy, M. *Chem. Eng. News* **1999**, *77*, 10.
(5) Saraf, M. K.; Gerard, S.; Wojcinski, L. M., II; Charpentier, P. A.; DeSimone, J. M.; Roberts, G. W. *Macromolecules* **2002**, *35*, 7976−7985.
(6) Saraf, M. K.; Wojcinski, L. M., II; Kennedy, K. A.; Gerard, S.; Charpentier, P. A.; DeSimone, J. M.; Roberts, G. W. *Macromol. Symp.* **2002**, *182*, 119−129.
(7) Charpentier, P. A.; Kennedy, K. A.; DeSimone, J. M.; Roberts, G. W. *Macromolecules* **1999**, *32*, 5973−5975.
(8) Charpentier, P. A.; DeSimone, J. M.; Roberts, G. W. *Ind. Eng. Chem. Res.* **2000**, *39*, 4588−4596.
(9) Galia, A.; Caputo, G.; Spadaro, G.; Filardo, G. *Ind. Eng. Chem. Res.* **2002**, *41*, 5934−5940.
(10) Mueller, P. A.; Storti, G.; Morbidelli, M.; Apostolo, M.; Martin, R. *Macromolecules* **2005**, *38*, 7150−7163.
(11) Chatzidoukas, C.; Pladis, P.; Kiparissides, C. *Ind. Eng. Chem. Res.* **2003**, *42*, 743−751.
(12) Tai, H.; Wang, W.; Martin, R.; Liu, J.; Lester, E.; Licence, P.; Woods, H. M.; Howdle, S. M. *Macromolecules* **2005**, *38*, 355−363.
(13) Tai, H.; Wang, W.; Howdle, S. M. *Macromolecules* **2005**, *38*, 1542−1545.
(14) Galia, A.; Giaconia, A.; Scialdone, O.; Apostolo, M.; Filardo, G. *J. Polym. Sci., Part A: Polym. Chem.* **2006**, *44*, 2406−2418.
(15) Strain, F.; Bissinger, W. E.; Dial, W. R.; Rudoff, H.; DeWitt, B. J.; Stevens, H. C.; Langston, J. H. *J. Am. Chem. Soc.* **1950**, *72*, 1254−1263.
(16) Galia, A.; Giaconia, A.; Iaia, V.; Filardo, G. *J. Polym. Sci., Part A: Polym. Chem.* **2004**, *42*, 173−185.
(17) Scialdone, O.; Galia, A.; Raimondi, S.; Filardo, G. *J. Supercrit. Fluids* **2006**, http://dx.doi.org/10.1016/j.supflu.2006.03.012.
(18) Vilenchik, L. Z.; Rubinsztajn, S.; Zeldin, M.; Fife, W. K. *J. Polym. Sci., Part B: Polym. Phys.* **1991**, *29*, 1137−1140.
(19) Lutringer, G.; Weill, G. *Polymer* **1991**, *32*, 877−883.
(20) Hsiao, Y. L.; Maury, E. E.; DeSimone, J. M.; Mawson, S.; Johnston, K. P. *Macromolecules* **1995**, *28*, 8159−8166.
(21) O'Neill, M. L.; Yates, M. Z.; Johnston, K. P.; Smith, C. D.; Wilkinson, S. P. *Macromolecules* **1998**, *31*, 2838−2847.
(22) Canelas, D. A.; DeSimone, J. M. *Macromolecules* **1997**, *30*, 5673−5682.
(23) Mueller, P. A.; Storti, G.; Morbidelli, M. *Chem. Eng. Sci.* **2005**, *60*, 377−397.
(24) Mueller, P. A.; Storti, G.; Morbidelli, M. *Chem. Eng. Sci.* **2005**, *60*, 1911−1925.
(25) Fehrenbacher, U.; Muth, O.; Hirth, T.; Ballauff, M. *Macromol. Chem. Phys.* **2000**, *201*, 1532−1539.
(26) Fehrenbacher, U.; Ballauff, M. *Macromolecules* **2002**, *35*, 3653−3661.
(27) Kumar, S.; Ramkrishna, D. *Chem. Eng. Sci.* **1996**, *51*, 1311−1332.
(28) Kumar, S.; Ramkrishna, D. *Chem. Eng. Sci.* **1996**, *51*, 1333−1342.
(29) Kumar, S.; Ramkrishna, D. *Chem. Eng. Sci.* **1997**, *52*, 4659−4679.
(30) Lepilleur, C.; Beckman, E. J. *Macromolecules* **1997**, *30*, 745−756.

MA060981L